A Generalized Multicarrier Communication System – Part I: Theoretical Performance Analysis and Bounds

Imran Ali
self@ImranAliPhD.com
Independent Researcher, Melbourne, Australia

Abstract
This paper develops a generalized framework for the analysis of multicarrier communication system, using a generic pair of transmitters- and receiver side terraforms, $\boldsymbol{Q}_T \mid \boldsymbol{Q}_R$, such that the DFT-transform based "conventional OFDM" is its special case. This analysis framework is then used to propose and prove theorems on various performance metrics of a multicarrier communication system, which will apply to any system that fits the architecture, which most will do. The analysis framework also derives previously unknown closed-form expressions for these metrics, such as how the performance degradation due to carrier frequency offset or timing synchronization error, amongst others, are function of generic transforms. While extensive work exists on the impact of these challenges on conventional OFDM, how are these functions of transform matrices is unknown in the literature. It will be shown, how the analysis of OFDM based system is special case of analysis in this paper. This paper is Part I of three paper series, where the other two supplements the arguments present here.
Keywords:
OFDM, Multicarrier, Transforms, PAPR, Equalisation.

1. Introduction

The multicarrier modulation and more specifically, orthogonal frequency division multiplexing (OFDM), is the choice of fifth generation (5G) wireless communication standard [1], as well multiple other industry standards, including IEEE 802.11 (commonly known as WiFi) [2]. Because of this popularity, there is vast literature covering every aspect of this transmission scheme. However, the popularity of OFDM comes as a two-faced sword: on one hand, OFDM is has attractive features, such as efficient use of channel bandwidth [3], single-tap equalization [4] that allows low complexity receiver design and relative robustness to timing synchronisation errors [5]. On the other hand, OFDM suffers from high peak to average power ratio (PAPR) [6] and its inability to harvest channel diversity like single carrier system can, thereby incurring performance penalty, as well as sensitivity to frequency offset [7].

To address these drawbacks of the OFDM transmission, numerous approaches have been proposed for each its challenges. However, it is remarkable that, considering the body of OFDM literature, little (for example [8]-[10]) has been said about designing alternative transforms (as opposed to conventional Fourier transforms) by expressing various metrics of multicar carrier communication (MC) system performance as a function of these transforms, thereby allowing us to optimize the transforms before these challenges arise. This paper is an endeavour in that direction. Specifically, the paper aims to design a novel alternative transform pair, with a generalised matrix $\boldsymbol{Q}_T$ used at transmitter and matrix $\boldsymbol{Q}_R$ at receiver, hereafter referred to as $\boldsymbol{Q}_T \mid \boldsymbol{Q}_R$ pair in this paper, and seek to express the performance metrics of such a generalized multicarrier system (GMC) as a function of these matrices. The paper seeks to derive closed form expressions for relationship between $\boldsymbol{Q}_T \mid \boldsymbol{Q}_R$ pair and performance metrics. To the end, this paper expresses PAPR performance, sensitivity to timing synchronization and frequency offset, bit error rate (BER) performance, complexity of equalization and expression for per-subcarrier signal to noise ratio (SNR) as a function $\boldsymbol{Q}_T \mid \boldsymbol{Q}_R$ pair of matrices.

It should be noted that, while a generalised $\boldsymbol{Q}_T \mid \boldsymbol{Q}_R$ pair will not lend itself to the interpretation of sub-carriers, like the DFT-based conventional OFDM does, the terminology of sub-carriers is still retained in the context of $\boldsymbol{Q}_T \mid \boldsymbol{Q}_R$, albeit in the mathematical sense. More specifically, at a baseband level conventional OFDM, the Fourier transform of constellation mapped symbols is just the multiplication of DFT matrix to the vector of complex symbols, yielding another vector of complex symbols, which is still true in the case of $\boldsymbol{Q}_T$.

A. Contribution of this Paper

In the following, the contributions of this paper are summarized.

1) A generalized mathematical framework, with $\boldsymbol{Q}_T \mid \boldsymbol{Q}_R$ as respectively the transmitter and receiver side unitary matrices, is proposed such that every multicarrier commutation system is its special case.
2) *Theorem 1* proposes and proves closed form expression for PAPR of GMC as a function of generic $\boldsymbol{Q}_T$ matrix.
3) *Theorem 2* proposes design principles on $\boldsymbol{Q}_T \mid \boldsymbol{Q}_R$ that can avoid BER performance penalty in the presence of certain timing synchronization errors.

Manuscript received September 5, 2024
Manuscript revised September 20, 2024
https://doi.org/10.22937/IJCSNS.2024.24.9.1

4) Two novel closed form expressions for SINR with $\boldsymbol{Q}_T \mid \boldsymbol{Q}_R$ pair for both zero-forcing and MMSE equalisation are presented. It is shown that, unlike conventional OFDM, the two are *not* identical for all $\boldsymbol{Q}_T \mid \boldsymbol{Q}_R$ pair.
5) For a given carrier frequency offset (CFO), a novel closed-form expression for SINR impact on CFO for any $\boldsymbol{Q}_T \mid \boldsymbol{Q}_R$ is also derived.

B. *Limitation of this paper*

Due to the sheer breadth of scope of this paper, the analysis and results of this paper are limited to simpler baseband model with single transmitter-side and single receiver-side antenna. The generalisation to MIMO-based transmission and other architectures is beyond the scope of this paper.

2. Mathematical Model of GMC

In this section, the mathematical analysis framework for the GMC system is presented. This system is shown in Figure 1. Much like the conventional OFDM, the vector $\boldsymbol{X}$, containing symbols from a normalized square Quadrature amplitude modulation (QAM) alphabet, $\mathcal{A}$, is multiplied with transmitter side matrix, $\boldsymbol{Q}_T$, followed by the insertion of cyclic prefix (CP) of length L_P, so that $\boldsymbol{x}_{\text{cp}}$ is transmitted over Raleigh fading wireless channel, such that after removal of CP, the resulting channel matrix, $\boldsymbol{H}_c$, is circulant. At the receiver, the receiver-side transform $\boldsymbol{Q}_R$ is applied. Before we delve inoto receiver side, let formalize the transform pair.

Since the $\boldsymbol{Q}_T \mid \boldsymbol{Q}_R$ pair is the subject of optimization in this paper, they are kept as generic as possible with minimal assumptions on their structure. More specifically, in order to be used in the GMC system, while still preserving as much generality as possible, the $\boldsymbol{Q}_T \mid \boldsymbol{Q}_R$ pair must satisfy the following two conditions:

1) $\boldsymbol{Q}_T$ should not change the power of the transmit vector $\boldsymbol{X}$, i.e., $\|\boldsymbol{Q}_T\boldsymbol{X}\|^2 = \|\boldsymbol{X}\|^2$, which is equivalent to saying that the $\boldsymbol{Q}_T$ should be unitary, i.e., $\boldsymbol{Q}_T^{\mathcal{H}}\boldsymbol{Q}_T = \boldsymbol{I}_N$, where $(.)^{\mathcal{H}}$ is the Hermitian transpose of argument.
2) $\boldsymbol{Q}_R$ is inverse of $\boldsymbol{Q}_T$, i.e., $\boldsymbol{Q}_R\boldsymbol{Q}_T = \boldsymbol{I}_N$. Then, from (i), $\boldsymbol{Q}_T^{\mathcal{H}} = \boldsymbol{Q}_R$.

In the remainder of this paper, only the two conditions given above are assumed on the $\boldsymbol{Q}_T \mid \boldsymbol{Q}_R$ pair. It should also be noticed that the OFDM precoding can be assumed to be merged with the $\boldsymbol{Q}_T \mid \boldsymbol{Q}_R$ pair, so that the discussion and optimization of alternative transform also applies to that of alternative precoding in many respects because the matrix product is unique.

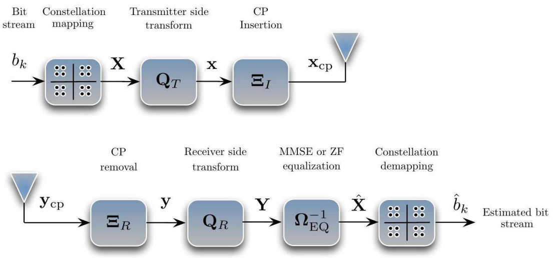

Figure 1: Transmitter and receiver block diagram of GMC

Returning to our signal model, except where otherwise specified, the CFO and timing errors are considered to be zero in this section. In such case, after the application of $\boldsymbol{Q}_R$, the zero-forcing equalization can be applied with multiplication of $\boldsymbol{\Omega}^{-1}$, which a diagonal matrix for conventional OFDM (the specific conditions on $\boldsymbol{Q}_T \mid \boldsymbol{Q}_R$ pair that will allow single-tap equalization will be formulated in *Theorem 3*). Under such conditions, the estimate at the receiver for the transmitted vector $\boldsymbol{X}$ with ZF equalization is given as

$$\begin{aligned}\hat{\boldsymbol{X}} &= (\boldsymbol{Q}_R\boldsymbol{H}_c\boldsymbol{Q}_T)^{-1}\boldsymbol{Q}_R\boldsymbol{H}_c\boldsymbol{Q}_T\boldsymbol{X} + (\boldsymbol{Q}_R\boldsymbol{H}_c\boldsymbol{Q}_T)^{-1}\boldsymbol{Q}_R\boldsymbol{\eta} \\ &= \boldsymbol{Q}_R\boldsymbol{H}_c^{-1}\boldsymbol{Q}_T\boldsymbol{Q}_R\boldsymbol{H}_c\boldsymbol{Q}_T\boldsymbol{X} + \boldsymbol{Q}_R\boldsymbol{H}_c^{-1}\boldsymbol{Q}_T\boldsymbol{Q}_R\boldsymbol{\eta} \\ &= \boldsymbol{X} + \boldsymbol{Q}_R\boldsymbol{H}_c^{-1}\boldsymbol{\eta}, \end{aligned} \tag{1}$$

where $\boldsymbol{\Omega}^{-1} = (\boldsymbol{Q}_R\boldsymbol{H}_c\boldsymbol{Q}_T)^{-1}$ is the ZF equalization matrix and $\boldsymbol{\eta}$ is zero mean white Gaussian noise with mean $\mu_{[\boldsymbol{\eta}]_k} \triangleq E\{[\boldsymbol{\eta}]_k\} = 0$ and $\sigma^2_{[\boldsymbol{\eta}]_k} = N_o, \forall k$, where $\sigma^2_{\{\cdot\}}$ is the variance of quantity in the subscript.

3. Bounds on PAPR Performance

From the very definition of PAPR, it is easy to see that the expression for PAPR is given as,

$$\gamma^{\text{GMC}} \triangleq \frac{\max\limits_i\left\{\max\limits_n\left\{\left|\left[\boldsymbol{x}_{\text{cp},i}\right]_n\right|^2\right\}\right\}}{\frac{1}{N+L_P}E\|\boldsymbol{x}_{\text{cp},i}\|^2}, \tag{2}$$

which is a function of transmitter side matrix because $\boldsymbol{x}_{\text{cp}}$ is cyclic prefixed version of $\boldsymbol{x} = \boldsymbol{Q}_T\boldsymbol{X}$. In what follows, *Theorem 1* formulates the PAPR of GMC system and finds upper and lower bounds on it. But before we present the theorem, following Lemma is required.

Lemma 1. If $[a_0, a_1, \dots, a_{N-1}]$ is a row or a column of a unitary matrix, therefore with the property $\sum_{n=0}^{N-1}|a_n|^2 = 1$, then the following upper bounds are satisfied

$$\left(\sum_{n=0}^{N-1}|a_n|\right)^2 \leq N, \text{ and } \sum_{n=0}^{N-1}|a_n| \leq \sqrt{N}.$$

Proof. The reader can easily verify *Lemma 1* using simple algebraic manipulations. ■

The parts (***a***) and (***b***) of the following theorem summarize the result for the PAPR of GMC system for a square QAM.

Theorem 1 (*PAPR of square QAM GMC system*): If $\boldsymbol{Q}_T$ is the $N \times N$ sized transmitter-side matrix of a GMC system, used to transmit complex symbols from a normalized square QAM alphabet $\mathcal{A}$ with $A_{\max}^2 = \max_k |[\mathcal{A}]_k|^2$, then,

a) the PAPR of the GMC system, γ^{GMC}, is as given in Equation (3),

$$\gamma^{GMC} = \frac{A_{\max}^2}{2} \max_n \left\{ \left| \sum_{m=0}^{N-1} g[\boldsymbol{Q}_T]_{n,m} \right|^2 \right\} \quad (3)$$

where $g \in \{\pm 1 \pm j\}$,

b) the PAPR of GMC, γ^{GMC}, satisfies the following bound:

$$A_{\max}^2 \le \gamma^{GMC} \le N A_{\max}^2, \quad (4)$$

where $A_{\max}^2$ is the maximum power of any symbol in the QAM alphabet, $\mathcal{A}$.

Proof. To prove ***(a)***, from Equation (2), the expression for the *instantaneous* PAPR for the i^{th} GMC symbol is given as

$$\gamma_i^{\text{GMC}} \triangleq \max_i \gamma_i^{\text{GMC}} = \frac{\max_i \left\{ \max_n \left\{ \left| \left[\boldsymbol{x}_{\text{cp},i} \right]_n \right|^2 \right\} \right\}}{\frac{1}{N + L_P} E \left\| \boldsymbol{x}_{\text{cp},i} \right\|^2}. \quad (5)$$

The peak power will not change before and after CP insertion because the CP consists of the entries of the symbol itself, so the numerator in Equation (5), which is also the instantaneous peak power, γ_i^{peak}, can be computed as

$$\begin{aligned} \gamma_i^{\text{peak}} &= \max_i \left\{ \max_n \{ |[\boldsymbol{x}_i]_n|^2 \} \right\} \\ &= \max_i \left\{ \max_n \left\{ \left| \sum_{m=0}^{N-1} [\boldsymbol{Q}_T]_{n,m} [\boldsymbol{X}_i]_m \right|^2 \right\} \right\}. \end{aligned} \quad (6)$$

The peak power occurs when all the entries of $\boldsymbol{X}_i$ are one of the maximum power symbols from alphabet $\mathcal{A}$, i.e., $[\boldsymbol{X}_i]_n \in \{a | a \in \mathcal{A} |a|^2 =, A_{\max}^2\}$. QAM constellations, that are square and normalised, have 4 different symbols with the maximum power of $A_{\max}^2$. These symbols are $\frac{A_{\max}}{\sqrt{2}} + j\frac{A_{\max}}{\sqrt{2}}, \frac{A_{\max}}{\sqrt{2}} - j\frac{A_{\max}}{\sqrt{2}}, -\frac{A_{\max}}{\sqrt{2}} + j\frac{A_{\max}}{\sqrt{2}}$ and $-\frac{A_{\max}}{\sqrt{2}} - j\frac{A_{\max}}{\sqrt{2}}$. Therefore, when $[\boldsymbol{X}_i]_m \in \left\{ g\frac{A_{\max}}{\sqrt{2}}; g \in \{\pm 1 \pm j\} \right\}, \forall\, i, m$, the power of the i^{th} GMC symbol will spike to its maximum value, and in such case the maximization over i can be dropped. This leads to

$$\begin{aligned} \gamma^{\text{peak}} &= \max_n \left\{ \left| \frac{A_{\max}}{\sqrt{2}} \sum_{m=0}^{N-1} g[\boldsymbol{Q}_T]_{n,m} \right|^2 \right\} \\ &= \frac{A_{\max}^2}{2} \max_n \left\{ \left| \sum_{m=0}^{N-1} g[\boldsymbol{Q}_T]_{n,m} \right|^2 \right\}. \end{aligned} \quad (7)$$

To compute average power,

$$\begin{aligned} \gamma_{\text{avg}} &= \frac{1}{N + L_P} E \|\boldsymbol{x}_{\text{cp},i}\|^2 \\ &= \frac{1}{N + L_P} \frac{N + L_P}{N} E \|\boldsymbol{x}_i\|^2 \\ &= \frac{1}{N} E\{\|\boldsymbol{Q}_T \boldsymbol{X}_i\|^2\} \\ &= \frac{1}{N} E\{\|\boldsymbol{X}_i\|^2\} = 1, \end{aligned} \quad (8)$$

where second step in Equation (8) follows because the power increases by $\frac{N+L_P}{N}$ after CP insertion and 4th step follows because the multiplication by a unitary matrix preserves the norm and that the constellation $\mathcal{A}$ is normalized, i.e., since $[\boldsymbol{X}_i]_n \in \mathcal{A}$ and $\frac{1}{M} \sum_k |[\mathcal{A}]_k|^2 = 1$, so $E\|\boldsymbol{X}_i\|^2 = N$.

Thus, using Equations (7) and (8), the PAPR of GMC system becomes that which was given in Equation (3),

$$\gamma^{\text{GMC}} = \frac{A_{\max}^2}{2} \max_n \left\{ \left| \sum_{m=0}^{N-1} g[\boldsymbol{Q}_T]_{n,m} \right|^2 \right\}$$

which concludes the proof of part ***(a)***.

To prove part ***(b)*** of the theorem, start by noting that, for N complex numbers, $a_0, a_1, \dots, a_{N-1} \in \mathbb{C}$, it is easy to verify that

$$\left| \sum_{n=0}^{N-1} a_n \right|^2 \le \left(\sum_{n=0}^{N-1} |a_n| \right)^2 \quad (9)$$

Using Equation (9) in the PAPR expression for the GMC in Equation (8) leads to an upper bound given by

$$\begin{aligned} \gamma^{\text{GMC}} &\le \frac{A_{\max}^2}{2} \max_n \left\{ \left(\sum_{m=0}^{N-1} |g[\boldsymbol{Q}_T]_{n,m}| \right)^2 \right\} \\ &= \frac{A_{\max}^2}{2} \max_n \left\{ \left(\sum_{m=0}^{N-1} |g||[\boldsymbol{Q}_T]_{n,m}| \right)^2 \right\} \\ &= A_{\max}^2 \max_n \left\{ \left(\sum_{m=0}^{N-1} |[\boldsymbol{Q}_T]_{n,m}| \right)^2 \right\} \\ &= N A_{\max}^2, \end{aligned} \quad (10)$$

which is the upper bound on PAPR, where third step in Equation (10) is obtained by $|g|^2 = |\pm 1 \pm 1|^2 = 2$ and then by using *Lemma 1*, the inequality (10) follows.

To see the lower bound, for N complex number $a_0, a_1, \dots, a_{N-1} \in \mathbb{C}$, it can be said that

$$\left|\sum_{p=0}^{N-1} a_p\right|^2 = \sum_{p=0}^{N-1} |a_p|^2 + 2\Re\mathrm{e}\left\{\sum_{p=0}^{N-2}\sum_{p=q+1}^{N-1} a_p a_q^*\right\} \triangleq \sum_{p=0}^{N-1} |a_p|^2 + \kappa, \quad (11)$$

where $\kappa \triangleq 2\Re\mathrm{e}\{\sum_{p=0}^{N-2}\sum_{p=q+1}^{N-1} a_p a_q^*\}$ has been defined, with $\Re\mathrm{e}\{\cdot\}$ being the real part of the quantity in the argument. It can be seen that $\kappa \geq 0$ because, by the definition of absolute value, $|\sum_p a_p|^2 \geq 0$ and $\sum_p |a_p|^2 \geq 0$. Since $|\sum_m^{N-1} g[\boldsymbol{Q}_T]_{n,m}|^2 \geq 0$, using Equation (11) into Equation (3), the PAPR expression for GMC now reduces to

$$\begin{aligned}\gamma^{\mathrm{GMC}} &= \frac{A_{\max}^2}{2}\left(\max_n\left\{\sum_{m=0}^{N-1} |g[\boldsymbol{Q}_T]_{n,m}|^2\right\} + \max_n\{\kappa\}\right)\\ &= \frac{A_{\max}^2}{2}\left(\max_n\left\{\sum_{m=0}^{N-1} |g|^2|[\boldsymbol{Q}_T]_{n,m}|^2\right\} + \max_n\{\kappa\}\right)\\ &= A_{\max}^2\left(\max_n\left\{\sum_{m=0}^{N-1} |[\boldsymbol{Q}_T]_{n,m}|^2\right\} + \max_n\{\kappa\}\right)\\ &= A_{\max}^2\left(1 + \max_n\{\kappa\}\right)\\ &\geq A_{\max}^2 \end{aligned} \quad (12)$$

where $|g|^2 = 2$ has been used in third step of Equation (12) and fourth step of Equation (12) follows because $\boldsymbol{Q}_T$ is a unitary matrix with unit norm for n^{th} row, $\forall n$. This concludes the proof of part ***(b)***. ■

3.1 Special Case: Conventional OFDM

The PAPR of conventional OFDM is known in the literature to be $NA_{\max}^2$ (see, for example, [11]). This can be easily derived from GMC expression in *Theorem 1* by substituting $\boldsymbol{Q}_T = \boldsymbol{F}^{\mathcal{H}}$ in Equation (3) and using $n = 0$, so that $[\boldsymbol{F}]_{0,m} = \frac{1}{\sqrt{N}}, \forall m$, then the PAPR on the 0^{th} is,

$$\gamma_{n=0}^{\mathrm{OFDM}} = \frac{A_{\max}^2}{2}\max_{\pm}\left\{\left|\sum_{m=0}^{N-1} g[\boldsymbol{F}^{\mathcal{H}}]_{0,m}\right|^2\right\} = \frac{A_{\max}^2}{2N}\max_{\pm}\left|\sum_{m=0}^{N-1} g\right|^2 = NA_{\max}^2, \quad (13)$$

which is also the upper bound on PAPR, so we do not need to consider other value of n. Thus, when it comes to PAPR, the conventional OFDM is the *worst possible system*, and any arbitrary unitary matrix will either match its PAPR or beat it. In the Part II and III papers [12], [13] of this series, we will present $\boldsymbol{Q}_T$ that have better PAPR performance.

4. Performance Bounds due to Timing Errors

For conventional OFDM, the timing synchronization error and resulting loss of SNR is we well established in the literature [5]. Specifically, let ζ, L and L_P be respectively the synchronization error, channel length and CP length, all in number of samples, then if $L_P - L \leq \zeta \leq 0$, a condition that is easy to satisfy in practice as CP length is parameter that can be tuned, then the conventional OFDM is penalised with an easily correctable offset, without any severe performance degradation due to inter symbol interference (ISI). This section aims to seek a $\boldsymbol{Q}_R \mid \boldsymbol{Q}_T$ pair, if any, which, when $L_P - L \leq \zeta \leq 0$, also avoids ISI. The case where the bounds on ζ mention above are not satisfied are beyond the scope of this paper and would be rare in real world cases.

It should be emphasized here, and will be proved shortly, that, even if $L_P - L \leq \zeta \leq 0$ is true, not every $\boldsymbol{Q}_R \mid \boldsymbol{Q}_T$ pair will avoid the ISI and resulting performance loss. The reason a DFT based conventional OFDM system incurs only a phase rotation, rather than an ISI, is because of the CP and cyclic nature of DFT transform. However, it is shown here that this property is not strictly limited to DFT, and it can be generalized for certain matrices.

Definition (Periodicity of a Matrix or Sequence): Consider an $N \times N$ matrix $\boldsymbol{Q}$ such that its $(u, v)^{th}$ entry is a function of u and v, i.e., $[\boldsymbol{Q}]_{u,v} \triangleq f(u, v), \forall u, v$. The matrix $\boldsymbol{Q}$ is referred to in this paper as row-wise N-periodic (respectively column-wise N-periodic) if $f(u + pN, v) = f(u, v)$ (respectively $f(u, v + pN) = f(u, v)$), where p is an integer. Furthermore, if $\boldsymbol{Q}$ is both row-wise and column-wise N-periodic, it is referred to simply as N-periodic matrix. Further to that, a sequence (vector), with $[\boldsymbol{Q}]_u = f(u)$, is N-periodic if $f(u + pN) = f(u)$, where p is an integer.

The DFT matrix, for example, is N-periodic because

$$\begin{aligned}[\boldsymbol{F}]_{u+qN,v+pN} &= \frac{1}{\sqrt{N}}e^{-j\frac{2\pi}{N}(u+qN)(v+pN)}\\ &= \frac{1}{\sqrt{N}}e^{-j\frac{2\pi}{N}uv} \cdot e^{-j2\pi u} \cdot e^{-j2\pi pv} \cdot e^{-j2\pi p}\\ &= \frac{1}{\sqrt{N}}e^{-j\frac{2\pi}{N}uv} = [\boldsymbol{F}]_{u,v}. \end{aligned} \quad (14)$$

Lemma 2 (Hermitian Transpose and Periodicity). For two $N \times N$ matrices $\boldsymbol{Q}_1$ and $\boldsymbol{Q}_2$, if $\boldsymbol{Q}_1$ is N-periodic matrix and $\boldsymbol{Q}_2 \triangleq \boldsymbol{Q}_1^{\mathcal{H}}$, then $\boldsymbol{Q}_2$ is also N-periodic.

Proof. The goal is to show that, for any two integers p and q, $[\boldsymbol{Q}_2]_{u+p\ \ ,v+qN} = [\boldsymbol{Q}_2]_{u,v}$. Since $\boldsymbol{Q}_2 = \boldsymbol{Q}_1^{\mathcal{H}}$, it can be said that

$$\begin{aligned}[\boldsymbol{Q}_2]_{u+pN,v+qN} &= [\boldsymbol{Q}_1]^{\mathcal{H}}_{v+qN,u+pN} \\ &= [\boldsymbol{Q}_1]^{\mathcal{H}}_{v,u} \ (\because \boldsymbol{Q}_1 \text{ is } N\text{-periodic}) \\ &= [\boldsymbol{Q}_2]_{u,v} \end{aligned} \quad (15)$$

which concludes the proof. ■

Lemma 3. If $\boldsymbol{Q}_1$ and $\boldsymbol{Q}_2$ are two N-periodic matrices, then their product is always N-periodic.

Proof. The product of two N-periodic matrices $\boldsymbol{Q}_1$ and $\boldsymbol{Q}_2$ is given by

$$\begin{aligned}[\boldsymbol{Q}]_{u,v} &\triangleq \sum_{k=0}^{N-1} [\boldsymbol{Q}_1]_{u,k}[\boldsymbol{Q}_2]_{k,v} \\ \Rightarrow [\boldsymbol{Q}]_{u+pN,v+qN} &= \sum_{k=0}^{N-1} [\boldsymbol{Q}_1]_{u+pN,k}[\boldsymbol{Q}_2]_{k,v+qN} \\ &= \sum_{k=0}^{N-1} [\boldsymbol{Q}_1]_{u,k}[\boldsymbol{Q}_2]_{k,v} = [\boldsymbol{Q}]_{u,v} \end{aligned} \quad (16)$$

which concludes the proof. ■

The *Lemmas 2* and *3* build towards formalization of the following about the impact of timing synchronization errors on the performance of GMC.

Theorem 2 (Timing Synchronization Errors and ISI). If the timing synchronization error of ζ samples is introduced into a GMC system with receiver-side transform $\boldsymbol{Q}_R$, if the condition, $L_P - L \leq \zeta \leq 0$, holds then no inter-symbol interference (ISI) will be incurred if $\boldsymbol{Q}_R$ satisfies *one* of the following conditions:

a) $\boldsymbol{Q}_R$ is N-periodic and $[\boldsymbol{Q}_R]_{u,v+\zeta} = g\big(K_u, [\boldsymbol{Q}_R]_{u,v}\big)$, where K_u is independent of v but same for all entries of u^{th} row, and $g(\cdot,\cdot)$ is an arithmetic operation between the arguments, or

b) the $\boldsymbol{Q}_R$ itself does not satisfy condition (***a***) but it can be expressed as $\boldsymbol{Q}_R = \tilde{\boldsymbol{Q}}_R \boldsymbol{\Psi}$, where $\tilde{\boldsymbol{Q}}_R$ satisfies condition (***a***) and $\boldsymbol{\Psi}$ is N-periodic.

Proof. To prove part $(\boldsymbol{a})$, recall the sampled vector of size $(N + L_P) \times 1$ before CP removal, $\boldsymbol{x}_{\text{cp}} = \Xi_I \boldsymbol{Q}_T \boldsymbol{X}$, where Ξ_I is the CP insertion matrix. Let the start of $\boldsymbol{x}_{\text{cp}}$ has been estimated to be ζ earlier such that $L_P - L \leq \zeta \leq 0$, so that the k^{th} sample of shifted vector is denoted as $[\bar{\boldsymbol{x}}_{\text{cp}}]_k \triangleq [\boldsymbol{x}_{\text{cp}}]_{k-\zeta}$. After the removal of CP, since the estimate of start of symbol is attained ζ samples earlier, the last ζ samples of the CP will still be at the start of the new CP-removed symbol, whereas last ζ samples of the new CP-removed symbol will be lost to subsequent symbol. After CP removal, let $[\bar{\boldsymbol{x}}]_k \triangleq [\boldsymbol{x}]_{k-\zeta}$ and since the CP is taken from the end of the symbol, the first ζ samples of $\bar{\boldsymbol{x}}$ are actually the last ζ samples of $\boldsymbol{x}$. This structure of $\bar{\boldsymbol{x}}$ is valid for all $\boldsymbol{Q}_T \mid \boldsymbol{Q}_R$ pairs if the CP has been used.

After $\boldsymbol{Q}_R$ transform of ζ samples shifted vector, the u^{th} entry of resultant vector, denoted in this paper as $[\boldsymbol{X}^{\odot\zeta}]_u$, is given as

$$[\boldsymbol{X}^{\odot\zeta}]_u = \sum_{v=0}^{N-1} [\boldsymbol{Q}_R]_{u,v}[\boldsymbol{x}]_{v-\zeta}. \quad (17)$$

Let $p = v - \zeta$ such that, when v goes from 0 for $N-1, p$ goes to $-\zeta$ to $N-1-\zeta$. Then from Equation (17)

$$[\boldsymbol{X}^{\odot\zeta}]_u = \sum_{p=-\zeta}^{N-1-\zeta} [\boldsymbol{Q}_R]_{u,p+\zeta}[\boldsymbol{x}]_p \quad (18)$$

such that if the matrix $\boldsymbol{Q}_R$ satisfies condition in (***a***) of theorem, then

$$[\boldsymbol{X}^{\odot\zeta}]_u = \sum_{p=-\zeta}^{N-1-\zeta} g\big(K_u, [\boldsymbol{Q}_R]_{u,p}\big)[\boldsymbol{x}]_p \quad (19)$$

where $g(a,b)$ is any arithmetic operation between a and b, where $a, b \in \mathbb{C}$, such that

$$[\boldsymbol{X}^{\odot\zeta}]_k = \begin{cases} \sum_{p=-\zeta}^{N-1-\zeta} K_u[\boldsymbol{Q}_R]_{u,p}[\boldsymbol{x}]_p = K_u[\boldsymbol{X}]_k, & \text{if } g(a,b) = ab \\ \sum_{p=-\zeta}^{N-1-\zeta} \frac{1}{K_u}[\boldsymbol{Q}_R]_{u,p}[\boldsymbol{x}]_p = \frac{1}{K_u}[\boldsymbol{X}]_k, & \text{if } g(a,b) = \frac{a}{b} \\ \sum_{p=-\zeta}^{N-1-\zeta} (K_u + [\boldsymbol{Q}_R]_{u,p})[\boldsymbol{x}]_p = [\boldsymbol{X}]_k + K_u \sum_{p}^{N-1} [\boldsymbol{x}]_p, & \text{if } g(a,b) = a+b \\ \sum_{p=-\zeta}^{N-1-\zeta} (K_u - [\boldsymbol{Q}_R]_{u,p})[\boldsymbol{x}]_p = [\boldsymbol{X}]_k - K_u \sum_{p}^{N-1} [\boldsymbol{x}]_p, & \text{if } g(a,b) = a-b \end{cases} \quad (20)$$

In either case, the additive or multiplicative quantity from $\boldsymbol{X}_k$ can be removed easily with single arithmetic operation. In conventional OFDM, this is done by offset correction, as elaborated after the proof.

It should be emphasized here that if $(u,v)^{\text{th}}$ entry of $\boldsymbol{Q}_R$ can not be separated from $[\boldsymbol{Q}_R]_{u,v+\zeta}, \forall u, v$, by some K_u, which is same for all u but independent of v, the $\boldsymbol{Q}_R$ and $\boldsymbol{Q}_T$ will not invert each other and $\boldsymbol{X}$ cannot be obtained.

To see the proof of part ***(b)***, since $\boldsymbol{\Psi}$ is periodic, $\boldsymbol{x}_{\Psi} \triangleq \boldsymbol{\Psi}\boldsymbol{x}$ is also periodic. Then since $\boldsymbol{Q}_R = \tilde{\boldsymbol{Q}}_R \boldsymbol{\Psi}$, it can be seen that

$$[\boldsymbol{X}]_k = [\tilde{\boldsymbol{Q}}_R \boldsymbol{x}_\Psi]_k = \sum_{n=0}^{N-1} [\tilde{\boldsymbol{Q}}_R]_{k,n} [\boldsymbol{x}_\Psi]_n$$

$$\begin{aligned}[\boldsymbol{X}^{\odot\zeta}]_k &= \sum_{n=0}^{N-1} [\tilde{\boldsymbol{Q}}_R]_{k,n} [\boldsymbol{x}_\Psi]_{n-\zeta} \\ &= \sum_{p=-m}^{N-1-\zeta} [\tilde{\boldsymbol{Q}}_R]_{k,p+\zeta} [\boldsymbol{x}_\Psi]_p \qquad \text{(by letting } p = n-\zeta) \\ &= \sum_{p=-\zeta}^{N-1-\zeta} g\left(K, [\tilde{\boldsymbol{Q}}_R]_{k,p}\right) [\boldsymbol{x}_\Psi]_p \end{aligned} \tag{21}$$

For all arithmetic operations between a and b, the Equation (23) at the bottom of this page provide value for $[\boldsymbol{X}^{\odot\zeta}]_k$, where again the additive or multiplicative quantities from $[\boldsymbol{X}]_k$ can be removed easily. This concludes the proof. ■

4.1 Special Case: Conventional OFDM

It is easy to check that the DFT matrix satisfies the condition $(\boldsymbol{a})$ in *Theorem 2* and hence the conventional OFDM avoids the ISI. In particular, for conventional OFDM,

$$\begin{aligned}[\boldsymbol{F}]_{u,v+\zeta} &= \frac{1}{\sqrt{N}} e^{-j\frac{2\pi}{N}u(v+\zeta)} \\ &= \frac{1}{\sqrt{N}} e^{-j\frac{2\pi}{N}(uv+u\zeta)} = \frac{1}{\sqrt{N}} e^{-j\frac{2\pi}{N}uv} e^{-j\frac{2\pi}{N}u\zeta} \\ &= [\boldsymbol{F}]_{u,v} K_u \end{aligned} \tag{22}$$

where, as required in the theorem, $K_u \triangleq e^{-j\frac{2\pi}{N}u\zeta}$ is independent of v but same for all entries of u^{th} row.

5. Equalization: Complexity Performance

In the GMC system, equalization can be performed either at the receiver (i.e., post-equalization) or at the transmitter (i.e., pre-equalization). In the latter case, channel state information (CSI) is required at the transmitter. Furthermore, unlike conventional OFDM where the ZF and MMSE equalizers have same error performance, for the GMC system, it is not necessarily the same for the two equalization approaches. The focus of this section is the complexity of equalization operation, especially single-tap equalization, which is one of the most famous aspects of conventional OFDM.

As the name suggests, the single-tap equalization mitigates the effects of the channel using just a single multiplication per subcarrier. *Theorem 3* asserts that [8], of all the possible $\boldsymbol{Q}_T \mid \boldsymbol{Q}_R$ pairs, only the DFT and matrices obtained from its row / column permutation pair, can enable single tap equalisation.

Theorem 3 (Single-Tap Equalization for GMC): In a CP based GMC system, only the DFT transform pair (and transform pairs obtained by rearranging the columns or rows of DFT pair) can enable single-tap equalization.

Proof. For a GMC system with transform pair $\boldsymbol{Q}_T \mid \boldsymbol{Q}_R$ and circulant channel matrix, $\boldsymbol{H}_c$, the equivalent channel response matrix before equalization is given as

$$\boldsymbol{\Omega} = \boldsymbol{Q}_R \boldsymbol{H}_c \boldsymbol{Q}_T = \boldsymbol{Q}_R \boldsymbol{F}^{\mathcal{H}} \boldsymbol{D} \boldsymbol{F} \boldsymbol{Q}_T \tag{23}$$

where $\boldsymbol{D} \triangleq \boldsymbol{F}\boldsymbol{H}_c\boldsymbol{F}^{\mathcal{H}} \Rightarrow \boldsymbol{H}_c = \boldsymbol{F}^{\mathcal{H}} \quad \boldsymbol{D}\boldsymbol{F}$ has been used. Defining $\boldsymbol{G}^{\mathcal{H}} \triangleq \boldsymbol{Q}_R\boldsymbol{F}^{\mathcal{H}} \Rightarrow \boldsymbol{G} = \boldsymbol{F}\boldsymbol{Q}_T$ and using it in Equation (23) leads to

$$\boldsymbol{\Omega} = \boldsymbol{G}^{\mathcal{H}} \boldsymbol{D} \boldsymbol{G} \tag{24}$$

Since both $\boldsymbol{Q}_R$ and $\boldsymbol{F}^{\mathcal{H}}$ are unitary, $\boldsymbol{G}^{\mathcal{H}}$ is also unitary with $\boldsymbol{G}$ being its inverse. Given that $\boldsymbol{D}$ is diagonal, Equation (24) shows a eigenvalue decomposition (EVD) of matrix $\boldsymbol{\Omega}$.

Now, for single-tap equalization, the matrix $\boldsymbol{\Omega}$ should be diagonal, so define $\boldsymbol{\Omega} \triangleq \boldsymbol{D}'$, where $\boldsymbol{D}'$ is diagonal. In such case, since the eigenvalues of a diagonal matrix are entries in its own diagonal, the diagonals of matrices $\boldsymbol{D}'$ and $\boldsymbol{D}$ contain same entries but not necessarily in the same order.

Let $[\boldsymbol{e}]_{\cdot,j}$ denote an eigenvector of matrix $\boldsymbol{D}'$ corresponding to its j^{th} eigenvalue, then all the entries of $[\boldsymbol{e}]_{\cdot,j}$ are zero except the j^{th} entry, which is 1.

$$[\boldsymbol{X}^{\odot\zeta}]_k = \begin{cases} \sum_{p=-\zeta}^{N-1-\zeta} K_u [\tilde{\boldsymbol{Q}}_R \boldsymbol{\Psi}\boldsymbol{x}]_{u,p} [\boldsymbol{x}_\Psi]_p = K_u [\boldsymbol{X}]_k & \text{if } g(a,b) = ab \\ \sum_{p=-\zeta}^{N-1-\zeta} \frac{1}{K_u} [\tilde{\boldsymbol{Q}}_R \boldsymbol{\Psi}\boldsymbol{x}]_{u,p} [\boldsymbol{x}_\Psi]_p = \frac{1}{K_u} [\boldsymbol{X}]_k & \text{if } g(a,b) = a/b \\ \sum_{p=-\zeta}^{N-1-\zeta} \left(K_u + [\tilde{\boldsymbol{Q}}_R \boldsymbol{\Psi}\boldsymbol{x}]_{u,p}\right) [\boldsymbol{x}_\Psi]_p = [\boldsymbol{X}]_k + K_u \sum_{p}^{N-1} [\boldsymbol{x}]_p & \text{if } g(a,b) = a+b \\ \sum_{p=-\zeta}^{N-1-\zeta} \left(K_u - [\tilde{\boldsymbol{Q}}_R \boldsymbol{\Psi}\boldsymbol{x}]_{u,p}\right) [\boldsymbol{x}_\Psi]_p = [\boldsymbol{X}]_k - K_u \sum_{p}^{N-1} [\boldsymbol{x}]_p, & \text{if } g(a,b) = a-b \end{cases} \tag{23}$$

The vectors $[\boldsymbol{e}]_{\cdot,j}, \forall j = 0,1,2,\dots,N-1$, are columns of $\boldsymbol{G}^{\mathcal{H}}$. Thus, $\boldsymbol{G}^{\mathcal{H}}$ and $\boldsymbol{G}$ have only one non-zero entry in each of their columns, which is 1. Therefore, they are permutation matrices with permutation order as per the order of the entries of $\boldsymbol{D}$.

Thus, to enable single-tap equalization, the $\boldsymbol{Q}_T \mid \boldsymbol{Q}_R$ pair becomes $\boldsymbol{G} = \boldsymbol{F}\boldsymbol{Q}_T \Rightarrow \boldsymbol{Q}_T = \boldsymbol{F}^{\mathcal{H}}\boldsymbol{G} \triangleq \boldsymbol{F}'^{\mathcal{H}}$ and $\boldsymbol{Q}_R = \boldsymbol{G}^{\mathcal{H}}\boldsymbol{F} \triangleq \boldsymbol{F}'$. The matrices $\boldsymbol{F}'^{\mathcal{H}}$ and $\boldsymbol{F}'$ are simply column and row permuted versions of $\boldsymbol{F}^{\mathcal{H}}$ and $\boldsymbol{F}$, respectively. Obviously, the standard DFT pair is one of these matrices. For a communication system, however, row or column permutation means rearranging subcarriers, which does not affect most, if not all, of the design and performance metrics of the system. This concludes the proof. ■

When the matrix $\boldsymbol{\Omega}$ is not diagonal, it can be subjected to some matrix manipulation schemes, for example, QR decomposition, that can produce easy to invert and implement matrices for each successive $\boldsymbol{H}_c$. This work is, however, beyond the scope of this paper.

5. Equalization: Error Performance

As will be seen in this section, the error performance of GMC depends not only on the $\boldsymbol{Q}_T \mid \boldsymbol{Q}_R$ pair but also on the equalization technique used. This contrasts to the conventional OFDM for which equalizers are identical.

5.1. Zero-Forcing Equalizer

The received vector for our GMC system is given as,

$$\boldsymbol{Y} = \boldsymbol{\Omega}\boldsymbol{X} + \boldsymbol{Q}_R\boldsymbol{\eta}. \tag{25}$$

where $\boldsymbol{\Omega} = \boldsymbol{Q}_R\boldsymbol{H}_c\boldsymbol{Q}_T$ is the equivalent channel transfer matrix, $\boldsymbol{\eta}$ is the noise vector, with its entries having zero mean and variance of $\frac{N_o}{2}$ per complex dimension, such that the total noise variance per noise sample is, $\sigma^2_{[\boldsymbol{\eta}]_k} = N_o, \forall k$.

Then, the ZF-equalization is carried out by pre-multiplying vector $\boldsymbol{Y}$ with the matrix $\boldsymbol{\Omega}_{\text{ZF}}^{-1} = (\boldsymbol{Q}_R\boldsymbol{H}_c\boldsymbol{Q}_T)^{-1} = \boldsymbol{Q}_R\boldsymbol{H}_c^{-1}\boldsymbol{Q}_T$, such that the estimate of vector $\boldsymbol{X}$ is given as

$$\begin{aligned}\hat{\boldsymbol{X}}_{\text{ZF}} &= \boldsymbol{X} + \boldsymbol{\Omega}_{\text{ZF}}^{-1}\boldsymbol{Q}_R\boldsymbol{\eta}\\ &= \boldsymbol{X} + \boldsymbol{e}\end{aligned} \tag{26}$$

where $\boldsymbol{e} \triangleq \boldsymbol{\Omega}_{\text{ZF}}^{-1}\boldsymbol{Q}_R\boldsymbol{\eta}$ is the estimation error.

5.1.1 SNR of k^{th} Subchannel of ZF-GMC

When $\hat{\boldsymbol{X}}_{\text{ZF}}$ is the ZF estimate of transmitted vector $\boldsymbol{X}$, then $\hat{\boldsymbol{X}}_{\text{ZF}} \triangleq \boldsymbol{X} + \boldsymbol{e}$, where the error vector, $\boldsymbol{e}$, is comprised entirely of noise due to ZF nature of equalization. The error, $\boldsymbol{e}$, is given as

$$\begin{aligned}\boldsymbol{e} &= \boldsymbol{\Omega}_{\text{ZF}}^{-1}\boldsymbol{Q}_R\boldsymbol{\eta} = (\boldsymbol{Q}_R\boldsymbol{H}_c^{-1}\boldsymbol{Q}_T)\boldsymbol{Q}_R\boldsymbol{\eta}\\ &= \boldsymbol{Q}_R(\boldsymbol{F}^{\mathcal{H}}\boldsymbol{D}^{-1}\boldsymbol{F})\boldsymbol{Q}_T\boldsymbol{Q}_R\boldsymbol{\eta}\\ &= \boldsymbol{Q}_R\boldsymbol{F}^{\mathcal{H}}\boldsymbol{D}^{-1}\boldsymbol{w}\end{aligned} \tag{27}$$

where $\boldsymbol{w} = \boldsymbol{F}\boldsymbol{\eta}$, with $\boldsymbol{w}$ retaining the mean and variance of $\boldsymbol{\eta}$, i.e. $E\{[\boldsymbol{w}]_k\} = 0$ and $\sigma^2_{[\boldsymbol{w}]_k} = N_o$. It should be noted that $[\boldsymbol{e}]_k, \forall k$, are still uncorrelated because all matrices being multiplied with $\boldsymbol{\eta}$ are unitary except $\boldsymbol{D}^{-1}$, which is diagonal. The output noise on k^{th} subchannel is given as

$$\begin{aligned}[\boldsymbol{e}]_k &= \sum_{n=0}^{N-1} [\boldsymbol{Q}_R\boldsymbol{F}^{\mathcal{H}}\boldsymbol{D}^{-1}]_{k,n}[\boldsymbol{w}]_n\\ &= \sum_{n=0}^{N-1} [\boldsymbol{Q}_R\boldsymbol{F}^{\mathcal{H}}]_{k,n}\frac{[\boldsymbol{w}]_n}{[\boldsymbol{D}]_{n,n}}\end{aligned} \tag{28}$$

where second equality follows because $\boldsymbol{D}^{-1}$ is diagonal. To compute noise power, the variance of $[\boldsymbol{e}]_k$ is needed. The terms in the summation in Equation (28) have 0 cross-correlation because $[\boldsymbol{w}]_k, \forall k$, are uncorrelated. Therefore, the variance of $[\boldsymbol{e}]_k$ is given by the sum of variances of these terms, i.e.,

$$\begin{aligned}\sigma^2_{[e]_k} &= \sum_{n=0}^{N-1} \text{var}\left\{[\boldsymbol{Q}_R\boldsymbol{F}^{\mathcal{H}}]_{k,n}\frac{[\boldsymbol{w}]_n}{[\boldsymbol{D}]_{n,n}}\right\}\\ &= \sum_{n=0}^{N-1} \left|[\boldsymbol{Q}_R\boldsymbol{F}^{\mathcal{H}}]_{k,n}\frac{[\boldsymbol{w}]_n}{[\boldsymbol{D}]_{n,n}}\right|^2,\end{aligned} \tag{29}$$

where the second equality follows because each term in the summation has zero mean because of $E\{[\boldsymbol{w}]_k\} = 0$. Therefore, the variance of noise on the k^{th} subchannel, $[\boldsymbol{e}]_k$, is given as

$$\begin{aligned}\sigma^2_{[e]_k} &= \sum_{n=0}^{N-1} \left|[\boldsymbol{Q}_R\boldsymbol{F}^{\mathcal{H}}]_{k,n}\right|^2 \frac{\sigma^2_{[\boldsymbol{w}]_n}}{\left|[\boldsymbol{D}]_{n,n}\right|^2}\\ &= N_o \sum_{n=0}^{N-1} \frac{\left|[\boldsymbol{Q}_R\boldsymbol{F}^{\mathcal{H}}]_{k,n}\right|^2}{\left|[\boldsymbol{D}]_{n,n}\right|^2}\\ &= N_o\psi_k,\end{aligned} \tag{30}$$

where $\psi_k \triangleq \sum_{n=0}^{N-1} \frac{\left|[\boldsymbol{Q}_R\boldsymbol{F}^{\mathcal{H}}]_{k,n}\right|^2}{\left|[\boldsymbol{D}]_{n,n}\right|^2}$. Using the least common multiple (LCM), ψ_k can be rewritten as

$$\psi_k = \frac{\sum_{n=0}^{N-1} \left|[\boldsymbol{Q}_R \boldsymbol{F}^{\mathcal{H}}]_{k,n}\right|^2 \prod_{m=0,m\neq n}^{N-1} \left|[\boldsymbol{D}]_{m,m}\right|^2}{\prod_{m=0}^{N-1} \left|[\boldsymbol{D}]_{m,m}\right|^2} \quad (31)$$

The SNR on the k^{th} subchannel of ZF equalized GMC system is thus given as

$$\beta_k^{\text{ZF,GMC}} = \frac{\sigma_{[X]_k}^2}{\sigma_{[e]_k}^2} = \frac{1}{N_o \psi_k}$$
$$= \beta_o \cdot \frac{\prod_{m=0}^{N-1} \left|[\boldsymbol{D}]_{m,m}\right|^2}{\sum_{n=0}^{N-1} \left(\left|[\boldsymbol{Q}_R \boldsymbol{F}^{\mathcal{H}}]_{k,n}\right|^2 \prod_{m=0,m\neq n}^{N-1} \left|[\boldsymbol{D}]_{m,m}\right|^2 \right)} \quad (32)$$

where $\beta_o \triangleq \frac{1}{N_o}$ is the pure AWGN channel SNR.

Equation (32) gives the SNR on the k^{th} subchannel of all ZF equalized MC systems as they are special cases of GMC system under consideration. A quick check can be made for conventional OFDM by substituting $\boldsymbol{Q}_R = \boldsymbol{F}$ in Equation (32), which readily leads to the well-known expression for the SNR on the k^{th} subcarrier of ZF equalized conventional OFDM, which is

$$\beta_k^{\text{ZF,OFDM}} = \beta_o \left|[\boldsymbol{D}]_{k,k}\right|^2. \quad (33)$$

Interestingly, the SNR for k^{th} subchannel of SC-FDE can still be deduced from the expression in Equation (32), giving credence to the notion that the position of equalization does not change the SNR and hence error performance. To obtain the SNR on the k^{th} subchannel of SCFDE, substitute $\boldsymbol{Q}_R = \boldsymbol{F}\boldsymbol{F}^{\mathcal{H}} = \boldsymbol{I}_N$ in Equation (32) to get

$$\beta_k^{\text{ZF,SC-F}} = \beta_o \cdot \frac{N \prod_{m=0}^{N-1} \left|[\boldsymbol{D}]_{m,m}\right|^2}{\sum_{n=0}^{N-1} \prod_{m=0,m\neq n}^{N-1} \left|[\boldsymbol{D}]_{m,m}\right|^2}$$
$$= \frac{N}{\sum_{n=0}^{N-1} \beta_o \left|[\boldsymbol{D}]_{n,n}\right|^2}, \quad (34)$$

which is same as that reported in the literature for SC-FDE [5], where second step in Equation (44) follows by dividing both numerator and denominator with $\prod_{m=0}^{N-1}\left|[\boldsymbol{D}]_{m,m}\right|^2$. It can also be noted that the SNR for the k^{th} subchannel of SC-FDE is independent of k, meaning that, for both ZF and MMSE equalizations, all the subchannels have identical SNR.

To find the relationship between the SNR of SC-FDE and conventional OFDM, multiply N times both numerator and denominator of Equation (34) with β_o so that m^{th} term in the products, $\beta_o[\boldsymbol{D}]_{m,m}\big|^2$, is the OFDM SNR on m^{th} subcarrier. This leads to relationship between SNR of conventional OFDM and SC-FDE as,

$$\beta_k^{\text{ZF,SC-FDE}} = N \left(\frac{\prod_{m=0}^{N-1} \beta_m^{\text{ZF,OFDM}}}{\sum_{n=0}^{N-1} \prod_{m=0,m\neq n}^{N-1} \beta_m^{\text{ZF,OFDM}}} \right). \quad (35)$$

5.2 MMSE Equalizer for GMC

Once again, starting from expression for $\boldsymbol{Y}$,

$$\boldsymbol{Y} = \boldsymbol{\Omega X} + \boldsymbol{Q}_R \boldsymbol{\eta}$$
$$\Rightarrow \hat{\boldsymbol{X}}_{\text{MMSE}} = \boldsymbol{\Omega}_{\text{MMSE}}^{-1} \boldsymbol{Y}$$
$$= \boldsymbol{X} + \boldsymbol{e} \quad (36)$$

where $\boldsymbol{\Omega}_{\text{MMSE}}^{-1}$ is the MMSE equalizer for which expression is to be derived here and $\boldsymbol{e}$ is the error vector after MMSE equalization, given as

$$\boldsymbol{e} = \hat{\boldsymbol{X}}_{\text{MMSE}} - \boldsymbol{X}$$
$$= \boldsymbol{\Omega}_{\text{MMSE}}^{-1} \boldsymbol{Y} - \boldsymbol{X} \quad (37)$$

By orthogonality principle for MMSE minimization, $\boldsymbol{e}$ should be orthogonal to observation vector $\boldsymbol{Y}$, i.e. $E\{\boldsymbol{e}\boldsymbol{Y}^{\mathcal{H}}\} = 0$. By using the value of $\boldsymbol{e}$ from Equation (37) to solve the orthogonality principle, the expression for MMSE can be derived as follows

$$E\{(\boldsymbol{\Omega}_{\text{MMSE}}^{-1} \boldsymbol{Y} - \boldsymbol{X})\boldsymbol{Y}^{\mathcal{H}}\} = 0$$
$$\Rightarrow \boldsymbol{\Omega}_{\text{MMSE}}^{-1} E\{\boldsymbol{Y}\boldsymbol{Y}^{\mathcal{H}}\} = E\{\boldsymbol{X}\boldsymbol{Y}^{\mathcal{H}}\}. \quad (38)$$

Substituting for $\boldsymbol{Y}$, we get $\boldsymbol{\Omega}_{\text{MMSE}}^{-1} E\{(\boldsymbol{\Omega X} + \boldsymbol{Q}_R \boldsymbol{\eta})(\boldsymbol{\Omega X} + \boldsymbol{Q}_R \boldsymbol{\eta})^{\mathcal{H}}\} = E\{\boldsymbol{X}(\boldsymbol{\Omega X} + \boldsymbol{Q}_R \boldsymbol{\eta})^{\mathcal{H}}\}$, thus

$$\boldsymbol{\Omega}_{\text{MMSE}}^{-1} E\{(\boldsymbol{\Omega X} + \boldsymbol{Q}_R \boldsymbol{\eta})((\boldsymbol{X\Omega})^{\mathcal{H}} + (\boldsymbol{\eta} \boldsymbol{Q}_R)^{\mathcal{H}})\}$$
$$= E\{\boldsymbol{X}((\boldsymbol{X\Omega})^{\mathcal{H}} + (\boldsymbol{\eta} \boldsymbol{Q}_R)^{\mathcal{H}})\} \quad (39)$$

By multiplying the brackets and using $E\{\boldsymbol{X}\boldsymbol{X}^{\mathcal{H}}\} = \boldsymbol{I}_N$, $E\{\boldsymbol{\eta}\boldsymbol{\eta}^{\mathcal{H}}\} = N_o \boldsymbol{I}_N$ and $E\{\boldsymbol{X}\boldsymbol{\eta}^{\mathcal{H}}\} = E\{\boldsymbol{\eta}\boldsymbol{X}^{\mathcal{H}}\} = \boldsymbol{O}_{N\times N}$ in Equation (39), the expression for MMSE is obtained as

$$\boldsymbol{\Omega}_{\text{MMSE}}^{-1}(\boldsymbol{\Omega}\boldsymbol{\Omega}^{\mathcal{H}} + N_o \boldsymbol{I}_N) = (\boldsymbol{\Omega}^{\mathcal{H}})$$
$$\Rightarrow \boldsymbol{\Omega}_{\text{MMSE}}^{-1} = (\beta_o \boldsymbol{\Omega}^{\mathcal{H}})(\beta_o \boldsymbol{\Omega}\boldsymbol{\Omega}^{\mathcal{H}} + \boldsymbol{I}_N)^{-1}$$
$$= (\beta_o \boldsymbol{Q}_R \boldsymbol{H}_c^{\mathcal{H}} \boldsymbol{Q}_T)(\beta_o \boldsymbol{Q}_R \boldsymbol{H}_c \boldsymbol{H}_c^{\mathcal{H}} \boldsymbol{Q}_T + \boldsymbol{I}_N)^{-1}. \quad (40)$$

Although Equation (40) gives a closed form expression for MMSE equalizer, it can be simplified further, which will be useful in, for example, finding the variance of noise.

In particular, if $\overline{\boldsymbol{H}}_c \triangleq \beta_o \boldsymbol{H}_c \boldsymbol{H}_c^{\mathcal{H}} + \boldsymbol{I}_N$ then it can be shown that $\beta_o \boldsymbol{Q}_R \boldsymbol{H}_c \boldsymbol{H}_c^{\mathcal{H}} \boldsymbol{Q}_T + \boldsymbol{I}_N = \boldsymbol{Q}_R \overline{\boldsymbol{H}}_c \boldsymbol{Q}_T$, and Equation (40) becomes,

$$\boldsymbol{\Omega}_{\text{MMSE}}^{-1} = (\beta_o \boldsymbol{\Omega}^{\mathcal{H}})(\boldsymbol{Q}_R \overline{\boldsymbol{H}}_c \boldsymbol{Q}_T)^{-1}$$
$$= (\beta_o \boldsymbol{Q}_R \boldsymbol{H}_c^{\mathcal{H}} \boldsymbol{Q}_T)(\boldsymbol{Q}_R \overline{\boldsymbol{H}}_c^{-1} \boldsymbol{Q}_T) \quad \text{(substituting } \boldsymbol{\Omega}^{\mathcal{H}}\text{)}$$
$$= \beta_o \boldsymbol{Q}_R \boldsymbol{H}_c^{\mathcal{H}} (\beta_o \boldsymbol{H}_c \boldsymbol{H}_c^{\mathcal{H}} + \boldsymbol{I}_N)^{-1} \boldsymbol{Q}_T \quad \text{(substituting } \overline{\boldsymbol{H}}_c\text{)}$$
$$= \beta_o \boldsymbol{Q}_R \boldsymbol{F}^{\mathcal{H}} \boldsymbol{D}^{\mathcal{H}} \boldsymbol{F} (\beta_o \boldsymbol{F}^{\mathcal{H}} \boldsymbol{D}\boldsymbol{D}^{\mathcal{H}} \boldsymbol{F} + \boldsymbol{I}_N)^{-1} \boldsymbol{Q}_T. \quad (\because\ \boldsymbol{H}_c = \boldsymbol{F}^{\mathcal{H}} \boldsymbol{D} \boldsymbol{F}) \quad (41)$$

Repeating the same process: if $\bar{\boldsymbol{D}} \triangleq \beta_o \boldsymbol{D}\boldsymbol{D}^{\mathcal{H}} + \boldsymbol{I}_N \Rightarrow \beta_o \boldsymbol{F}^{\mathcal{H}} \boldsymbol{D}\boldsymbol{D}^{\mathcal{H}} \boldsymbol{F} + \boldsymbol{I}_N = \boldsymbol{F}^{\mathcal{H}} \bar{\boldsymbol{D}} \boldsymbol{F}$, the simplified expression for MMSE equalizer can be obtained as

$$\begin{aligned}\boldsymbol{\Omega}_{\text{MMSE}}^{-1} &= \beta_o \boldsymbol{Q}_R \boldsymbol{F}^{\mathcal{H}} \boldsymbol{D}^{\mathcal{H}} \boldsymbol{F} (\boldsymbol{F}^{\mathcal{H}} \bar{\boldsymbol{D}} \boldsymbol{F})^{-1} \boldsymbol{Q}_T \\ &= \boldsymbol{Q}_R \boldsymbol{F}^{\mathcal{H}} [\beta_o \boldsymbol{D}^{\mathcal{H}} (\beta_o \boldsymbol{D}\boldsymbol{D}^{\mathcal{H}} + \boldsymbol{I}_N)^{-1}] \boldsymbol{F} \boldsymbol{Q}_T \\ &= \boldsymbol{Q}_R \boldsymbol{F}^{\mathcal{H}} \boldsymbol{P} \boldsymbol{F} \boldsymbol{Q}_T, \end{aligned} \tag{42}$$

where $\boldsymbol{P}$ is diagonal matrix with $[\boldsymbol{P}]_{u,u} \triangleq \frac{\beta_o [\boldsymbol{D}^{\mathcal{H}}]_{u,u}}{\beta_o [\boldsymbol{D}\boldsymbol{D}^{\mathcal{H}}]_{u,u} + 1}$.

5.2.1 SINR for MMSE-GMC System

Unlike the ZF equalizer, the MMSE equalizer will cause some ICI. This can be seen by noting that the matrix $\boldsymbol{\Omega}_{\text{ZF}}^{-1}$ is inverse of $\boldsymbol{\Omega}$, whereas the matrix $\boldsymbol{\Omega}_{\text{MMSE}}^{-1}$ is not. Therefore, the SINR is computed in this section. To that end, after the MMSE equalization, the estimate of the transmitted symbol vector is given as

$$\hat{\boldsymbol{X}} = \boldsymbol{\Omega}_{\text{MMSE}}^{-1} (\boldsymbol{\Omega} \boldsymbol{X} + \boldsymbol{Q}_R \boldsymbol{\eta}) \tag{43}$$

and the complex symbol on k^{th} subchannel is given as

$$\begin{aligned}[\hat{\boldsymbol{X}}]_k &= \underbrace{[\boldsymbol{\Omega}_{\text{MMSE}}^{-1} \boldsymbol{\Omega}]_{k,k}}_{\triangleq [\boldsymbol{a}]_k} [\boldsymbol{X}]_k + \underbrace{\sum_{\substack{n=0 \\ n \neq k}}^{N-1} [\boldsymbol{\Omega}_{\text{MMSE}}^{-1} \boldsymbol{\Omega}]_{k,n} [\boldsymbol{X}]_n}_{\triangleq [\boldsymbol{I}]_k} + \underbrace{\sum_{n=0}^{N-1} [\boldsymbol{\Omega}_{\text{MMSE}}^{-1} \boldsymbol{Q}_R]_{k,n} [\boldsymbol{\eta}]_n}_{\triangleq [\boldsymbol{w}_{\text{MMSE}}]_k} \\ &= [\boldsymbol{a}]_k [\boldsymbol{X}]_k + [\boldsymbol{I}]_k + [\boldsymbol{w}_{\text{MMSE}}]_k, \end{aligned} \tag{44}$$

where the three terms are signal, interference and noise components, respectively. To find the SINR on k^{th} subchannel, the variance of signal as well as variance of noise plus interference is required. However, since noise and interference are uncorrelated and $E\{|[\boldsymbol{X}]_k|^2\} = 1$, then SINR on the k^{th} subchannel is given as

$$\tilde{\beta}_k^{\text{GMC,MMSE}} = \frac{\sigma_{[\boldsymbol{a}]_k}^2}{\sigma_{[\boldsymbol{I}]_k}^2 + \sigma_{[\boldsymbol{w}_{\text{MMSE}}]_k}^2} \tag{45}$$

First, consider the MMSE-output noise, which is given as

$$\begin{aligned}\boldsymbol{w}_{\text{MMSE}} &= \boldsymbol{\Omega}_{\text{MMSE}}^{-1} \boldsymbol{Q}_R \boldsymbol{\eta} \\ &= \boldsymbol{Q}_R \boldsymbol{F}^{\mathcal{H}} \boldsymbol{P} \boldsymbol{F} \boldsymbol{Q}_T \boldsymbol{Q}_R \boldsymbol{\eta} \\ &= \boldsymbol{Q}_R \boldsymbol{F}^{\mathcal{H}} \boldsymbol{P} \boldsymbol{w} \end{aligned} \tag{46}$$

where $\boldsymbol{w} \triangleq \boldsymbol{F}\boldsymbol{\eta}$, such that $\boldsymbol{w}$ has same statistics as $\boldsymbol{\eta}$. On the other hand, $[\boldsymbol{w}_{\text{MMSE}}]_k, \forall k$, do not have same statistics as $[\boldsymbol{\eta}]_k$ but they are still uncorrelated because $\boldsymbol{Q}_R$ and $\boldsymbol{F}$ are unitary and $\boldsymbol{P}$ is diagonal. Since $\boldsymbol{P}$ is diagonal, the output noise on the k^{th} subchannel is given as

$$[\boldsymbol{w}_{\text{MMSE}}]_k = \sum_{n=0}^{N-1} [\boldsymbol{Q}_R \boldsymbol{F}^{\mathcal{H}}]_{k,n} [\boldsymbol{P}]_{n,n} [\boldsymbol{w}]_n \tag{47}$$

The mean of noise output noise is given as

$$\begin{aligned}\mu_{[\boldsymbol{w}_{\text{MMSE}}]_k} &= E\left\{\sum_{n=0}^{N-1} [\boldsymbol{Q}_R \boldsymbol{F}^{\mathcal{H}}]_{k,n} [\boldsymbol{P}]_{n,n} [\boldsymbol{w}]_n\right\} \\ &= \sum_{n=0}^{N-1} [\boldsymbol{Q}_R \boldsymbol{F}^{\mathcal{H}}]_{k,n} E\{[\boldsymbol{P}]_{n,n} [\boldsymbol{w}]_n\} = 0 \end{aligned} \tag{48}$$

because $E\{[\boldsymbol{P}]_{n,n} [\boldsymbol{w}]_n\} = 0$, as $\boldsymbol{P}$, a channel dependent quantity, and $\boldsymbol{w}$ are uncorrelated and $E\{[\boldsymbol{w}]_n\} = 0, \forall n$. Since $[\boldsymbol{w}_{\text{MMSE}}]_n, \forall n$, are uncorrelated, the variance of MMSE output noise is then given as

$$\begin{aligned}\sigma_{[\boldsymbol{w}_{\text{MMSE}}]_k}^2 &= E\{|[\boldsymbol{w}_{\text{MMSE}}]_k|^2\} \\ &= E\left\{\sum_{n=0}^{N-1} \left|[\boldsymbol{Q}_R \boldsymbol{F}^{\mathcal{H}}]_{k,n}\right|^2 \left|[\boldsymbol{P}]_{n,n}\right|^2 |[\boldsymbol{w}]_n|^2\right\} \\ &= N_o \sum_{n=0}^{N-1} \left|[\boldsymbol{Q}_R \boldsymbol{F}^{\mathcal{H}} \boldsymbol{P}]_{k,n}\right|^2 \end{aligned} \tag{49}$$

The interference term is given as

$$I_k = \sum_{\substack{n=0 \\ n \neq k}}^{N-1} [\boldsymbol{\Omega}_{\text{MMSE}}^{-1} \boldsymbol{\Omega}]_{k,n} [\boldsymbol{X}]_n \tag{50}$$

which, after putting value of $\boldsymbol{\Omega}_{\text{MMSE}}^{-1}$ and $\boldsymbol{\Omega}$ and few simplifications can be written as

$$I_k = \sum_{\substack{n=0 \\ n \neq k}}^{N-1} [\boldsymbol{Q}_R \boldsymbol{F}^H \boldsymbol{P} \boldsymbol{D} \boldsymbol{F} \boldsymbol{Q}_T]_{k,n} [\boldsymbol{X}]_n \tag{51}$$

which, for QAM alphabet $\mathcal{A}$, has zero mean, i.e. $\mu_{I_k} = 0$, because mean of a summation is the sum of means of individual terms. Furthermore, it can be shown that the terms in the summation in Equation (51) have zero covariance and therefore variance of interference term is sum of variance of individual terms in summation. Thus

$$\sigma_{I_k}^2 = \sum_{\substack{n=0 \\ n \neq k}}^{N-1} \left|[\boldsymbol{Q}_R \boldsymbol{F}^H \boldsymbol{P} \boldsymbol{D} \boldsymbol{F} \boldsymbol{Q}_T]_{k,n}\right|^2 \tag{52}$$

is the variance of the interference to the k^{th} subchannel. Thus, the SINR for that k^{th} subchannel is given as,

$$\tilde{\beta}_k^{\text{GMC,MMSE}} = \frac{|a_k|^2}{\sigma_{I_k}^2 + \sigma_{[w_{\text{MMSE}}]_k}^2} = \frac{\left|[\boldsymbol{Q}_R \boldsymbol{F}^{\mathcal{H}} \boldsymbol{PDFQ}_T]_{k,k}\right|^2}{\sum_{n=0,n\neq k}^{N-1} \left|[\boldsymbol{Q}_R \boldsymbol{F}^{\mathcal{H}} \boldsymbol{PDFQ}_T]_{k,n}\right|^2 + N_o \sum_{n=0}^{N-1} \left|[\boldsymbol{Q}_R \boldsymbol{F}^{\mathcal{H}} \boldsymbol{P}]_{k,n}\right|^2}. \quad (53)$$

A quick check can be performed here: it is well-known that the conventional OFDM has same SNR for both ZF and MMSE equalizers. To see this from Equation (53), put $\boldsymbol{Q}_T = \boldsymbol{F}^{\mathcal{H}}$ and $\boldsymbol{Q}_R = \boldsymbol{F}$ to get

$$\tilde{\beta}_k^{\text{GMC,MMSE}} = \frac{\left|[\boldsymbol{PD}]_{k,k}\right|^2}{\sum_{n=0,n\neq k}^{N-1} \left|[\boldsymbol{PD}]_{k,n}\right|^2 + N_o \sum_{n=0}^{N-1} \left|[\boldsymbol{P}]_{k,n}\right|^2} \quad (54)$$

Since $\boldsymbol{P}$ and $\boldsymbol{D}$ are both diagonal, $\sum_{n=0,n\neq k}^{N-1} \left|[\boldsymbol{PD}]_{k,n}\right|^2 = 0$. Therefore

$$\tilde{\beta}_k^{\text{GMC,MMSE}} = \frac{\left|[\boldsymbol{P}]_{k,k}\right|^2 \left|[\boldsymbol{D}]_{k,k}\right|^2}{N_o \left|[\boldsymbol{P}]_{k,k}\right|^2} = \beta_o \left|[\boldsymbol{D}_{k,k}]\right|^2, \quad (55)$$

which agrees with ZF SNR of OFDM derived in Equation (33).

6. Effect of CFO on GMC System Performance

In this section, an upper bound on the ICI power is derived for the GMC. The q^{th} entry of received vector (prior to $\boldsymbol{Q}_R$ transform) in the GMC system with a CFO (normalized by subcarrier width) of ϵ can be written as

$$[\boldsymbol{y}]_q = \sum_{n=0}^{N-1} e^{j\frac{2\pi}{N}q\epsilon} [\boldsymbol{h}]_l [\boldsymbol{x}]_{q-l} + [\boldsymbol{\eta}]_q \quad (56)$$

which, after defining a diagonal matrix $\boldsymbol{\Gamma}$ such that $[\boldsymbol{\Gamma}]_{q,q} = e^{j\frac{2\pi}{N}q\epsilon}$ can be written in matrix form as

$$\boldsymbol{y} = \boldsymbol{\Gamma H}_c \boldsymbol{Q}_T \boldsymbol{X} + \boldsymbol{\eta} \quad (57)$$

and following the receiver transform,

$$\Rightarrow \boldsymbol{Y} = \boldsymbol{Q}_R \boldsymbol{\Gamma H}_c \boldsymbol{Q}_T \boldsymbol{X} + \boldsymbol{Q}_R \boldsymbol{\eta}. \quad (58)$$

In the case of conventional OFDM, the CFO induced ICI is calculated from its Equation (58)-equivalent expression, $\boldsymbol{Y} = \boldsymbol{FH}_c \boldsymbol{F}^{\mathcal{H}} \boldsymbol{X} + \boldsymbol{F\eta}$, (i.e., $\boldsymbol{Q}_T = \boldsymbol{F}^{\mathcal{H}}, \boldsymbol{Q}_R = \boldsymbol{F}$ in Equation (58). For OFDM, $\boldsymbol{FH}_c \boldsymbol{F}^{\mathcal{H}}$ is diagonal but $\boldsymbol{F\Gamma H}_c \boldsymbol{F}^{\mathcal{H}}$ is not diagonal for $\epsilon \neq 0$, causing CFO-induced ICI among $[\boldsymbol{Y}]_p$, for all subcarrier p.

In the GMC framework, however, $\boldsymbol{Q}_R \boldsymbol{H}_c \boldsymbol{Q}_T$ is not necessarily assumed to be diagonal so as to maintain the generality of the system model for any $\boldsymbol{Q}_R \mid \boldsymbol{Q}_T$ pair. Therefore, Equation (58) can have ICI even if $\epsilon \neq 0$. So, to calculate ICI due to CFO alone, vector $\boldsymbol{Y}$ should be multiplied with $(\boldsymbol{Q}_R \boldsymbol{H}_c \boldsymbol{Q}_T)^{-1}$ first, i.e., ZF equalized, so that only CFO-induced ICI remains. It should be mentioned here that, if ϵ is known at receiver, equalization with $(\boldsymbol{Q}_R \boldsymbol{\Gamma H}_c \boldsymbol{Q}_T)^{-1}$ can eliminate CFO-induced ICI as well, but the goal of this section is to study the effect of CFO on GMC system, so $(\boldsymbol{Q}_R \boldsymbol{H}_c \boldsymbol{Q}_T)^{-1}$ is considered here.

Thus, after equalization, the estimate of the transmitted vector, $\hat{\boldsymbol{X}}$, is given as

$$\begin{aligned}\hat{\boldsymbol{X}} &= (\boldsymbol{Q}_R \boldsymbol{H}_c \boldsymbol{Q}_T)^{-1} \boldsymbol{Q}_R \boldsymbol{\Gamma H}_c \boldsymbol{Q}_T \boldsymbol{X} + (\boldsymbol{Q}_R \boldsymbol{H}_c \boldsymbol{Q}_T)^{-1} \boldsymbol{Q}_R \boldsymbol{\eta} \\ &= \boldsymbol{Q}_R \boldsymbol{H}_c^{-1} \boldsymbol{Q}_T \boldsymbol{Q}_R \boldsymbol{\Gamma H}_c \boldsymbol{Q}_T \boldsymbol{X} + \boldsymbol{Q}_R \boldsymbol{H}_c^{-1} \boldsymbol{Q}_T \boldsymbol{Q}_R \boldsymbol{\eta} \\ &= \boldsymbol{Q}_R \boldsymbol{H}_c^{-1} \boldsymbol{\Gamma H}_c \boldsymbol{Q}_T \boldsymbol{X} + \boldsymbol{Q}_R \boldsymbol{H}_c^{-1} \boldsymbol{\eta}. \end{aligned} \quad (59)$$

Noting that $\boldsymbol{D} = \boldsymbol{FH}_c \boldsymbol{F}^{\mathcal{H}} \Rightarrow \boldsymbol{H}_c = \boldsymbol{F}^{\mathcal{H}} \boldsymbol{DF}$ and $\boldsymbol{H}^{-1} = \boldsymbol{F}^{\mathcal{H}} \boldsymbol{D}^{-1} \boldsymbol{F}$ and putting it in Equation (59) leads to

$$\begin{aligned}\hat{\boldsymbol{X}} &= \boldsymbol{Q}_R \boldsymbol{F}^{\mathcal{H}} \boldsymbol{D}^{-1} \boldsymbol{F\Gamma F}^{\mathcal{H}} \boldsymbol{DFQ}_T \boldsymbol{X} + \boldsymbol{Q}_R \boldsymbol{F}^{\mathcal{H}} \boldsymbol{D}^{-1} \boldsymbol{F\eta} \\ &= \boldsymbol{G}^{\mathcal{H}} \boldsymbol{\Gamma G X} + \boldsymbol{G}^{\mathcal{H}} \boldsymbol{\eta}, \end{aligned} \quad (60)$$

where $\boldsymbol{G}^{\mathcal{H}} \triangleq \boldsymbol{Q}_R \boldsymbol{F}^{\mathcal{H}} \boldsymbol{D}^{-1} \boldsymbol{F}$, so that the estimate of k^{th} entry of transmitted vector is

$$\begin{aligned}[\hat{\boldsymbol{X}}]_k = \underbrace{[\boldsymbol{G}^{\mathcal{H}} \boldsymbol{\Gamma G}]_{k,k} [\boldsymbol{X}]_k}_{\triangleq [\boldsymbol{a}_\epsilon]_k,\ \text{signal}} + \underbrace{\sum_{\substack{i=0 \\ i\neq k}}^{N-1} [\boldsymbol{G}^{\mathcal{H}} \boldsymbol{\Gamma G}]_{k,i} [\boldsymbol{X}]_i}_{\triangleq [\boldsymbol{I}_\epsilon]_k,\ \text{CFO induced ICI}} \\ + \underbrace{\sum_{i=0}^{N-1} [\boldsymbol{G}^{\mathcal{H}}]_{k,i} [\boldsymbol{\eta}]_i}_{\triangleq [\boldsymbol{w}_\epsilon]_k,\ \text{noise}}. \end{aligned} \quad (61)$$

The SINR on the k^{th} subchannel in the presence of CFO is

$$\beta_k^{\text{CFO,GMC}} = \frac{\sigma_{[\boldsymbol{a}_\epsilon]_k}^2}{\sigma_{[\boldsymbol{I}_\epsilon]_k}^2 + \sigma_{[\boldsymbol{\eta}_\epsilon]_k}^2} \quad (62)$$

where $\sigma_{\{\cdot\}}^2$ denotes the variance of quantity in the subscript. Since the variance of each of these components is a function of $\boldsymbol{G}$, which is an interaction between the channel $\boldsymbol{D}$ and the transform matrix $\boldsymbol{Q}_T$, it may not be possible to find closed form expressions for these variances. It can be seen that if the knowledge of CSI is available to the transmitter, it can choose $\boldsymbol{Q}_R \boldsymbol{F}$ to whiten the channel effects and improve the worst-case ICI. Such investigation, however, is beyond the scope of this paper. In the case of conventional OFDM, the product $\boldsymbol{Q}_R \boldsymbol{F}$ is an identity matrix, which may be the cause of severe CFO induced performance degradation in the conventional OFDM system.

8. Conclusions

This paper focused on an MC systems based upon generic unitary transform matrices and addressed different aspects of such systems. In particular, the PAPR expression and a bound on it was derived, with an upper and lower bound on it as a function of $\boldsymbol{Q}_T$. The timing synchronization errors were studied for GMC system and its performance. The feasibility of single-tap equalization was also investigated, showing that only conventional OFDM can enable single-tap equalization. Furthermore, the expressions for ZF and MMSE equalizations and their SNR on each subchannel were also derived. The paper is aimed to serve as generic case for the systems considered in the subsequent papers in this series ([12], [13]).

The analysis framework developed in this paper is not only important for the design and investigation of alternative transform-based MC system, but it provides a common basis for the study of different existing MC systems, which are special cases of the system considered in the analysis framework.

References

[1] 3GPP. "5G; NR; Physical Channels and Modulation." 3rd Generation Partnership Project (3GPP), TS 38.211, v15.2.0, (2018).

[2] IEEE. "IEEE Standard for Technology—Telecommunications and Information Exchange Between Systems—Local and Metropolitan Area Networks—Specific Requirements—Part 11: Wireless LAN Medium Access Control (MAC) and Physical Layer (PHY) Specifications." IEEE Std 802.11-2016 (Revision of IEEE Std 802.11-2012), 1–3534, (2016).

[3] Sun, Y. "Bandwidth-Efficient Wireless OFDM." IEEE Journal on Selected Areas in Communications 19, no. 11 (2001): 2267–2278.

[4] Saltzberg, B. R. "Performance of an Efficient Parallel Data Transmission System." IEEE Transactions on Communication Technology 15, no. 6 (1967): 805–811.

[5] Peled, A., and A. Ruiz. "Frequency Domain Data Transmission Using Reduced Computational Complexity Algorithms." In Proceedings of IEEE International Conference on Acoustics, Speech, and Signal Processing (ICASSP), 964–967. Denver, CO, USA, April 1980.

[6] Bäuml, R. W., R. F. H. Fischer, and J. B. Huber. "Reducing the Peak-to-Average Power Ratio of Multicarrier Modulation by Selected Mapping." Electronics Letters 32, no. 22 (1996): 2056–2057.

[7] Moose, P. H. "A Technique for Orthogonal Frequency Division Multiplexing Frequency Offset Correction." IEEE Transactions on Communications 42, no. 10 (1994): 2908–2914.

[8] Ali, I., A. Pollok, L. Luo, and L. Davis. "A Low Complexity Receiver for T-Transform Based OFDM Systems." In Proceedings of IEEE 22nd International Symposium on Personal Indoor and Mobile Radio Communications, 1611–1615. Toronto, Canada, 2011.

[9] Ouyang, X., J. Jin, G. Jin, and P. Li. "Low Complexity Discrete Hartley Transform Precoded OFDM System Over Frequency-Selective Fading Channel." ETRI Journal 37, no. 1 (2015): 32–42.

[10] Ali, I., A. Pollok, L. Luo, and L. Davis. "A DHT Precoded OFDM System with Full Diversity and Low PAPR." In Proceedings of IEEE 23rd International Symposium on Personal Indoor and Mobile Radio Communications, 2383–2388. Sydney, Australia, 2012.

[11] Wang, Z., X. Ma, and G. B. Giannakis. "OFDM or Single-Carrier Block Transmissions?" IEEE Transactions on Communications 52, no. 3 (2004): 380–394.

[12] Ali, I. "A Generalized Multicarrier Communication System—Part II: The T-OFDM System." International Journal of Computer Science and Network Security 24, no. 9 (2024): 21–29.

[13] Ali, I. "A Generalized Multicarrier Communication System—Part III: Dual Symbol Superposition Block Carrier Transmission with Frequency Domain Equalization." International Journal of Computer Science and Network Security 24, no. 9 (2024): 41–49.

Dr. Imran Ali received the B.E. in Telecommunications from Mehran University of Engineering and Technology, Pakistan, an M.Sc. degree in Electronics and Communication Engineering from Myongji University, South Korea and PhD in Telecommunications from University of South Australia. Much of his academic research has been focused on signal processing for wireless communications. He is currently an independent researcher based in Melbourne, Australia.